

Scientific-Research Article

A Study on Lean, Sweep and Chord Length Effects on Aerodynamic Performance of Axial Fan of a High-bypass ratio Turbofan Engine

Amin Sarabchi¹, Mojtaba Heydarian², Ali Madadi^{3*}

^{1, 2, 3} - Faculty of Aerospace Engineering, Amirkabir University of Technology -

* Tehran, Postal code: 1591634311.

Email: *Ali.Madadi@aut.ac.ir

Compared to the enormous costs of laboratory experiments, numerical approaches to improving the performance of turbomachines are less costly and more practical. In the present study, by using the Taguchi method and orthogonal arrays while doing a limited number of simulations (according to the Taguchi method), the sensitivity level of objective functions have been investigated to optimization variables in a fan of a high-bypass ratio turbofan engine (JT9D-7 Engine). a mathematical parameterized algorithm coupled to a computational fluid dynamic solution is employed to modify the geometry and calculate the objective functions. 15 optimization variables are defined by varying:

a) The radial distribution of the chord length from the hub to the tip of the blade and also b) each profile's lean and sweep in five control points compared to hub profile.

The lean, sweep and chord length are parameterized by a spline algorithm. The objective functions included the pressure ratio, isentropic efficiency and mass flow rate of the fan in the design point. The results showed that the lean angle affects the isentropic efficiency, and the sweep angle affects the mass flow rate of the fan. The pressure ratio was sensitive to both variables. Concerning the design variables, 2-level L_{16} and L_{32} arrays of the Taguchi method were used for running the sensitivity analysis. Assuming a fixed number of blades, a fixed angle of incidence, and a fixed camber angle, distributing the chord length did not significantly affect the objective functions compared to the lean and sweep distribution.

Keywords: the Taguchi method, fan, lean, sweep, chord

Introduction

In order to develop the gas turbine industry in the field of aerospace, experience and technology in manufacturing are not sufficient and a strong knowledge of designing is essential for advancing the products of this industry based on the trending requirements. Due to the high expenses of empirical experiments, numerical methods are nowadays

much more practical and less costly than the former in improving the performance of turbomachinery. Using sensitivity analysis algorithms and optimization in designing has increased the efficiency of computations and decreased the number of repeated experiments and also lab high expenses. Optimization of this study's geometry includes the following stages:

¹ MA Student

² MA Degree

³ Assistant Professor (Corresponding Author)

1. Detecting the key parameters and eliminating and restricting the minor parameters.
2. Using Neural Network as a Predictive Model for outcomes in order to reduce the convergence time of the problem.
3. Effective optimization through the use of the genetic algorithm as an optimizer algorithm.

This study only presents the first part of the optimization problem and the outcomes of optimization will be demonstrated in future studies. Key parameters have been detected to reduce computational expenses and increase optimization efficiency. In fact, the sensitivity analysis that has been done is a stage of the optimization process that leads to the overall optimization through the use of the genetic algorithm. Design of experiment is a scientific approach through which objective changes are made in the influential factors playing in a process or product. Then the changes in the outcomes are examined. This examination gives us comprehensive information and an in-depth understanding of the process and product concerning the effect of the influential factors on the response or objective function. For determining the optimal combination of variables, researchers usually set different levels for every variable and examine every possible combination (full factorial) of variable levels. Assuming that N stands for the number of full factorial combinations, m stands for the number of variables, and L stands for the number of levels of each variable, then the following equation is reached:

$$N = L^m \quad (L > 2)$$

For example, if there are three variables in an examination and each has four levels, then 64 (4^3) combinations should be examined. If the number of m and L are not large, then examining up to the number of full factorials is reasonable. However, due to high computational expenses and being time-consuming, it is impossible to do many experiments. The Taguchi method is an economical approach to the design of experiment used (in the present study) to do the sensitivity analysis and detect the influential parameters before the optimization process. The initial population in the genetic algorithm and Neural Network is chosen randomly, but the Taguchi method has the privilege of generating the initial population for them. Detecting the key parameters and redefining the design parameters by employing the Taguchi method and

variance analysis before processing optimization by designing experiments familiarize us comprehensively with optimization variables. Wilson et al. (2012) redefined design parameters using the Taguchi method after parameterizing sweep angle along the blade span in optimal designing of a low-tone noise transonic fan.

Application of sensitivity assessment methods in investigating the effects of changing the geometry includes reducing computational costs, improving the prediction of turbomachines for increasing the performance, reducing the weight, decreasing flow losses, increasing pressure ratio, increasing stall margin, rotating stall avoidance, all of which can be accomplished by modifying the geometry of the blade.

In this sensitivity assessment of the axial fan blade, objective functions can be included isentropic efficiency, total pressure ratio, outlet pressure, pressure loss, weight, etc. The optimization variables can be included the blade's profile, camber angle and stacking line.

Literature Review

To provide a comprehensive look at the design variables and objective functions, an overview of studies and publications have been presented regarding designing and optimizing compressor blades and transonic fans. Much of the current advancement of research is due to NASA Rotor 37, a transonic compressor, and also the Rotor 67, a transonic fan. These two NASA's geometries have been used in 75 percent of the scholarly sources in this context and majority of researches from early 2000 to 2008, and following a subtle shift is seen.¹² Examining the advancement of research of this field, has been fallen into three different categories of scope, including 1) optimization of rotor 37 and rotor 67 2) optimization high loaded compressors 3) designing fan blades of aero-engine with high bypass ratio which are examined all the three respectively.

Using leaned and swept profiles is a common approach to modification of turbomachines' design to 3D design in order to improve the performance. Optimization is an effective tool in improving the objective functions of turbomachines. Several optimizations have been done by parameterizing the blade geometry concerning lean and sweep.

Denton et al. (2002) investigated the effects of leaned and swept blades on the performance of transonic fan of NASA Rotor 37 and 67.

Aerodynamic effects involved in improving the fan's performance based on shock-wave profile have been investigated. A 3D numerical solution on the flow field have been performed. Regarding the maximum efficiency of swept profiles, Denton et al. managed to extend the stall margin and also the performance area downstream.²

Benini (2004) used the genetic algorithm to run an aerodynamic analysis on the geometry of the blade of NASA Rotor 37. The study aimed at reaching the maximum of two objective functions, including the pressure ratio and isentropic efficiency in the design point with respect to the concept of lean and sweep. The study used Tascflow for numerical simulation. The results of this study indicated a 5.5 percent increase in the pressure ratio for only a 0.08 percent decrease in the isentropic efficiency.³

Oyama et al. (2004) optimized the transonic axial-flow blade through the evolutionary optimization algorithm based on the 3D feature of Reynolds-averaged Navier Stokes. To reduce the turnaround time of optimizing the geometry of NASA Rotor 67, a genetic algorithm coupled with a numerical code have been used. Modifying the blade's geometry concerning the concepts of lean and sweep increased the isentropic efficiency up to 2 percent.⁴

Jang et al. (2005) optimized a swept blade of an axial transonic compressor rotor. They used NASA Rotor 37 for geometry simulation. The flow field by 3D Navier Stokes equations have been analyzed. The optimization served to improve the isentropic efficiency and reduce the wastages of the shock wave. Their results indicated a 1.25 percent increase in the blade isentropic efficiency. The parting line between the shock wave and the boundary layer of suction surface moved downstream compared to the reference model.⁵

Samad et al. (2008) did a multiobjective optimization on an axial compressor with the geometry of NASA Rotor 37. Variations include the lean, sweep and skew of the blade stacking line. The research problem had two objective functions: the pressure ratio and the blade's isentropic efficiency. The flow field was solved by the 3D Reynolds-averaged Navier Stokes equations. The genetic algorithm (NSGA-II) was used for optimization. The optimization improved the pressure ratio and isentropic efficiency up to 1.25 percent and 0.51 percent, respectively.⁶

Razavi et al. (2014) did a numerical analysis on the lean and sweep angles of NASA Rotor 37. The aerodynamic behaviors based on the lean and sweep of the blade are investigated. The 3D Reynolds-

averaged Navier Stokes equations are used for solving the flow field problem. It was concluded that swept blades increase the overall area of performance up to 30 percent, isentropic efficiency up to 2 percent and pressure ratio up to 1 percent. In addition, leaned blades increase the safe area of performance up to 14 percent, isentropic efficiency up to 2 percent and pressure ratio up to 4 percent.⁷ Aerodynamic and structural design of transonic compressors with a high-pressure ratio (a stage higher than 1.8) is challenging and the existing design experience of these machines is limited. Thus, the optimization of these machines is of great importance. Siller et al. (2009, 2010) did an aerostructural optimization on one stage of a fan with a high-pressure ratio and one stator tandem. The optimization method was based on an evolutionary algorithm and accelerated by the sorting Kriging model. The CFD and CSM codes were used to evaluate the aerodynamic and structural performance. The constrained optimization problem was solved by two objective functions, including isentropic efficiency and stability margin, while mass flow rate and exit swirl angle were maintained.⁹

Neshat et al. (2015) investigated the blade sweep and lean effect in one stage of an industrial gas turbine's transonic compressor. Two geometries, one with a positive sweep and the other with a negative lean, were analyzed based on compressor design constraints. The first geometry increased the isentropic efficiency by 0.5 percent in the design point and the choking mass flow rate by 1.5 percent but decreased the stall margin. The second geometry increased the stall margin, the isentropic efficiency by 1 percent and the choking mass flow by 0.18 percent but decreased the compressor pressure ratio by 0.01 percent.¹⁰

Although the existing literature review has a considerable successful history of solving optimization problems modeling Rotor 37 and 67, only a few works aimed at optimizing the geometry of fan blades of large-sized turbofan engines with a high bypass ratio. Deng et al. (2013) optimized a high-bypass-ratio titanium blade of a turbofan of an engine both on the aerodynamic and aeromechanical sides. They implemented a multiobjective genetic algorithm connected to a Kriging model for the optimization. Design variables included swirl velocity (rV_θ) on the meridional channel of the blade, the spanwise distribution of the incidence angle, the maximum airfoil thickness and displacement of stacking line using the lean angle.

To make variations in the blade's geometry, 24 design variables were defined considering control points by implementing spline and Bezier functions. Both the aerodynamic and aeromechanical optimizations had two objective functions including the isentropic efficiency at design point and the slope of efficiency curve in the design rotational speed and at the point with 95% of design point mass flow rate. The aerodynamic optimization had two constraints and the aeromechanical one had nine. Both optimization approaches proved to have successful results. In the aerodynamic optimization, a 0.4 percent efficiency of the design point and a 0.8 percent increase in the efficiency of 95% point of the mass flow rate was achieved. In the aeromechanical optimization, the exact same points as in the aerodynamic optimization gained 0.2 and 0.67 percent of efficiency improvement, respectively.¹¹ Chahine (2018) in his Ph.D. thesis in the University of Oxford, aerostructurally optimized a fan blade using a Differential Evolution algorithm coupled to a Kriging model. This thesis first presents optimization of a titanium fan blade. Optimization variables include the chord length, the exit and inlet solid angles of the blade, airfoil thickness distribution, lean and sweep of the stacking line and the number of the blades. The spline function was used to distribute the blade angles (angle of tangent line to camber line and the machine's axis) among leading edge, trailing edge, and the middle point of the airfoil chord length in different spans. The spline function was also used to distribute the chord length, the blade thickness in each span, lean and sweep angle from the hub to the tip of the blade. However, a 2nd-degree bezier function is used to distribute the blade angle from the leading edge to the trailing edge in each span. The objective functions included maximum efficiency and stall margin of the cruise speed line. In this process, 12 aerodynamic and structural constraints were defined. After the optimization, the chord length increased and leading edge along the blade became forward-swept and the tip of the blade became backward-swept. For the final response choice among the Pareto Front points, The weight factor of the total efficiency parameter is considered larger than others. The design optimization with having all the defined constraints taken into account and eliminating two of the blades resulted in a 0.54 percent increase in the improvement of the efficiency and an insignificant improvement of stall margin.¹²

In the current study, the Taguchi algorithm coupled with Computational Fluid Dynamics is used to do a

3D sensitivity analysis on an axial fan blade. The database and arrays of the Taguchi method by Minitab software are established and generated the geometry mesh by TurboGrid software. The CFX software is used for numerical simulation and the Matlab platform for sensitivity analysis and automatic generation of geometry for the experiment. The sensitivity of the design was analyzed concerning three objective functions, including the total pressure ratio, the isentropic efficiency and the mass flow rate of the fan. The Fan geometry's lean and sweep angle and chord length are modified. The sensitivity of objective functions was investigated to variable changes and determined the areas of performance improvement of fan in design.

Numerical simulation of the axial fan

In the present study, the geometry of the axial fan of the JT9D-7 turbofan engine was modeled. Specifications of the blade are presented in Table 1.

Table 1 - Specifications of the axial fan ¹³

Pressure ratio	1.482
Mass flow rate (kg/s)	710
Root diameter to the tip of the entry	0.37
Number of blades	46
Blade's aspect ratio	4.6
Chord length of the root (cm)	15.32
Chord length of the tip (cm)	19.66

For generating the mesh, blockings H, C and O are used in order to divide the solution field for creating structured elements. Figure 1 shows the 2D blocking of the blade's profile, and Figure 2 depicts the structured mesh on the blade.

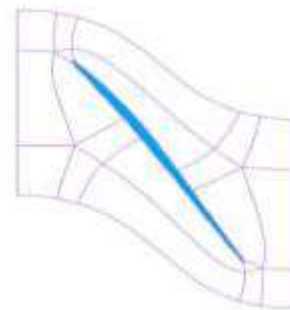


Figure 1 – 2D blocking of the blade's profile



Figure 2 – Meshing of the blade's 3D elements

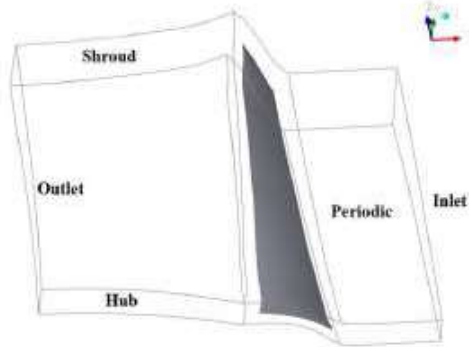


Figure 3 – Domain of the flow field and boundary conditions of the problem

In Figure 3, the domain of the flow field and the boundary conditions of the problem are shown. In order to reduce the computational cost, only one aerodynamic solution of the flow field was embedded for using its around periodic boundary conditions. Fan inlet airflow has the standard stagnation temperature and pressure (1 atmosphere and 288.15 Kelvin, respectively). Fan solution domain was rotating with the rotational speed of 3306 RPM. The static pressure of the blade outlet in the design point was set based on the pressure ratio of the design point (shown in Table 1) in a way that the stagnation pressure ratio of the design point would be maintained in the solution domain. The radial-equilibrium condition was considered and the static pressure value was set to the maximum radius of 113000 Pa. Due to the importance of the flow near the wall the two-equation SST $k-\omega$ model was used to simulate the turbulent flow around the blade. This model recognizes the transition of shear stresses and performs well in predicting the flow separation. So, as to do so, the mesh density around the wall must be high. This model does not employ any wall function near the wall. To stimulate the turbulent flow around the blade, Reynolds-averaged Navier Stokes equations were solved. Momentum, conservation of mass and energy equations were

iteratively solved to acquire the specifications of flow in the solution domain.

Figure 4 shows the distribution of Y^+ numbers around the blade in span 50%. The average value of Y^+ equals 1 and is located in the standard area of the SST turbulent model.¹⁴

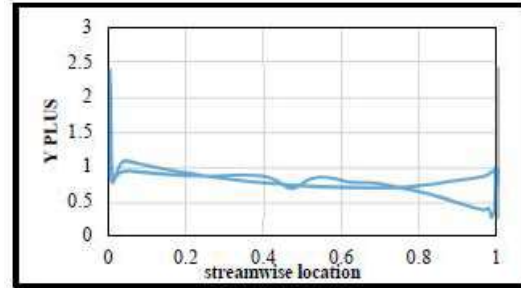


Figure 4 – Graph of Y^+ number of blade surface in the median span

Seven meshes were generated with 1.2 to 4 million elements to examine mesh independency of results. Figures 5 to 7 present the graphs of mesh independency.

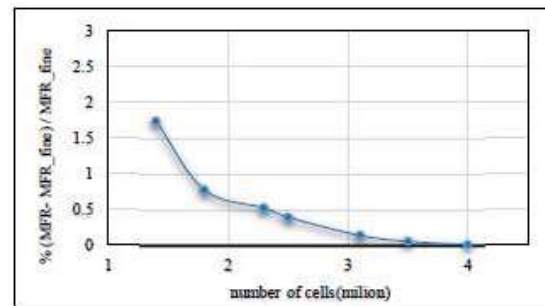


Figure 5 - Graph of examining mesh independency based on mass flow rate

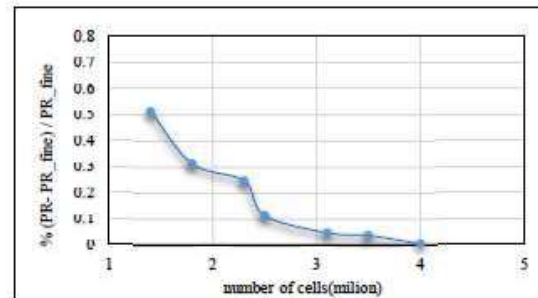


Figure 6 - Graph of examining mesh independency based on stagnation pressure ratio

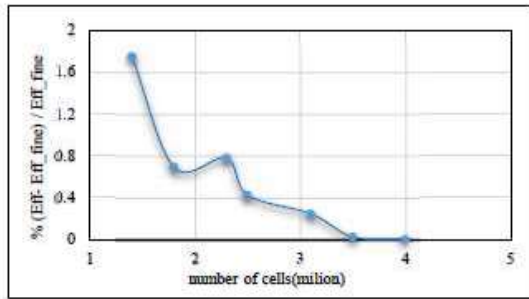


Figure 7 – Graph of examining mesh independency based on isentropic efficiency

Figures 8 and 9 present graphs of axial fan performance after generating a fine mesh with about 4 million elements. Figure 10 shows the contour of the Mach number in the span 50%. As shown in Figure 10, the shock wave was clearly created near the blade's leading edge. This shock wave became weak when reaching the stagnation point and weaker subsequently when the suction surface of the adjoining blade and the relative value of Mach number of the flow around the blade reached about 0.7. A 3D structure of the shock wave is shown in Figure 11. As it can be seen in this figure, the shock wave was created between span 50% and the blade tip. The location of the span 50 and 90 is shown.

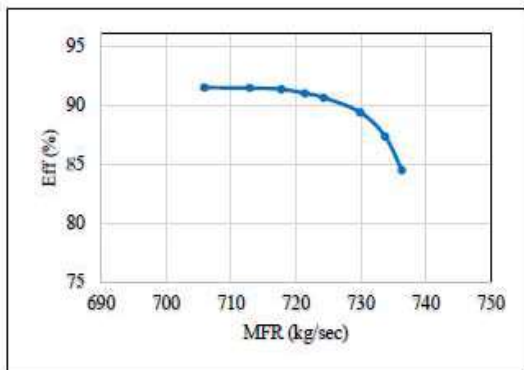


Figure 9 – Graph of efficiency based on mass flow rate

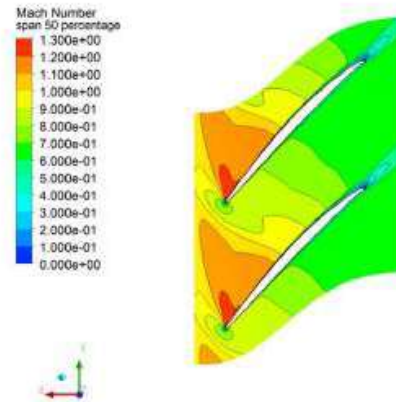


Figure 10 – Mach number contour in the Midspan

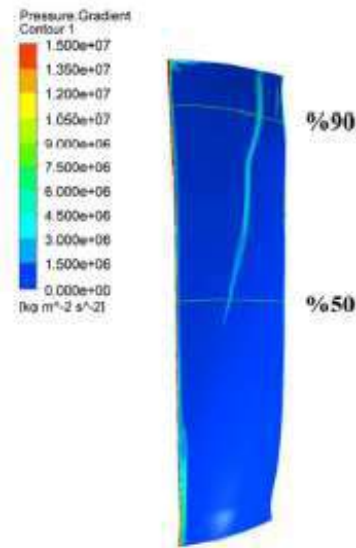


Figure 11 – contour of static pressure Gradient along the blade

Table 2 shows the difference between the numerical and experimental simulation results. To assess the reliability of performed, the mass flow rate and stagnation pressure ratio presented in Table 1, i.e., the results of fine mesh simulation, are compared to the data of the experimental method.

Table 2 – Comparison of experimental and numerical values¹³

Method	Mass flow rate (kg/s)	Pressure ratio	Efficiency
Experimental	710	1.482	-
Numerical	720.406	1.485	91.71
Percentage error	1.4	0.2	-

Table 3 presents the specifications of the blade of NASA Rotor 67. Since the experimental data of parameters of the fan blade is only available at the design point, the transonic NASA Rotor 67 is used to investigate the reliability of the CFD solution. Then, graphs depicting the specifications of this blade during the design were gained. Rotor 67 is a frequently-used blade in transonic fans and its geometry and experimental results are accurately documented. This rotor has 22 blades, and each blade's tip is 0.1016 cm far from the casing (1.1 percent of the tip chord length and 0.7 percent of the span length).¹⁶

Table 3 – Specification of NASA Rotor 67¹⁶

Speed of blade tip(m/s)	428.9
Inlet Relative Mach Number at the blade tip	1.38
Rotational speed (RPM)	16.43
Mass flow rate (kg/s)	33.25
Stagnation pressure ratio	1.63

Figures 12 and 13 show the performance in numerical simulation of the flow around the fan blade of Rotor 67 in addition to experimental data related to this at the design rotational speed.

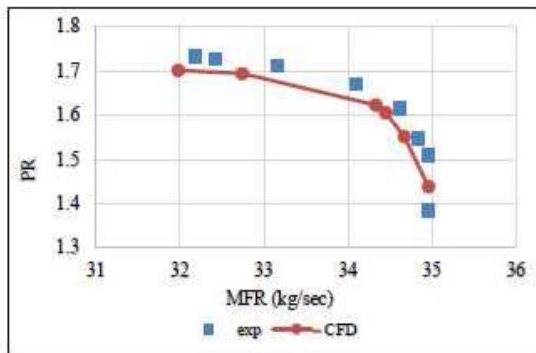


Figure 12 – Graph of pressure ratio based on mass flow rate of Rotor 67¹⁶

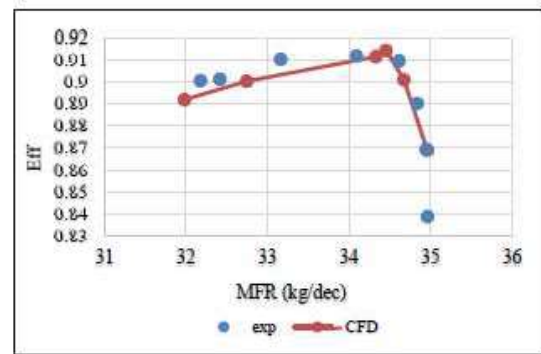


Figure 13 – Graph of isentropic efficiency based on mass flow rate of Rotor 67¹⁶

Design variables

The blade geometry was modified by changing the lean, sweep, and chord length amounts. The stacking line is created when the area center of each span of the blade is connected from the hub to the tip. If the stacking line moves downstream in the direction of the compressor axis while maintaining the blade chord length, there is a positive sweep. There is a negative sweep in the exact same situation if the line moves upstream. If the stacking line changes according to the direction of the rotation of the compressor blade while maintaining the blade chord length, there is a positive lean. In the exact same situation, there is a negative lean if the stacking line changes against the direction of the rotation of the compressor blade.⁵ Figure 14 shows the swept and leaned blades compared to the primary geometry of NASA Rotor 67.

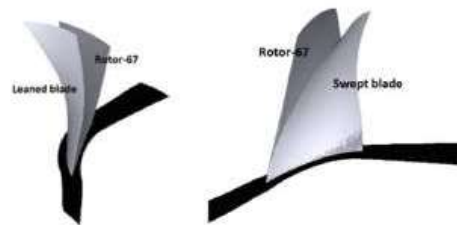


Figure 14 – Differences of the swept and leaned blades compared to the blade's primary geometry

The chord line of an airfoil is the line connecting the leading edge to the airfoil's trailing edge, and the chord length shows its quantity. As part of this study, the effect of chord distribution from the hub to the blade's tip is investigated on the objective functions. To maintain the amount of the camber and incidence angles of the flow fixed in relation to the blade and prevent any changes in the blade airfoil, a

scale factor was employed for enlargement and dwindlement. In every resizing of each blade span, all points of the airfoil were three-dimensionally enlarged and/or dwindled in relation to its area center. A spline function was used to distribute the scale factor from the hub to the tip of the blade. The research problem was parameterized by determining the stacking line and modifying it by the lean, sweep and chord line algorithms.

The spline algorithm was used to distribute the lean and sweep angles and the scale factor from the hub to the tip of the blade and for each of these three variables, five control points were considered in spans 20, 40, 60, 80 and 100 . Fifteen design variables were defined in total. The lean and sweep variables modify the blade stacking line, and the variables related to the scale factor modify the blade chord length in different spans. Table 4 presents the upper and lower bounds of the control points of the spline algorithm.

Table 4 - Bounds of the design variables

		Design variables				
		D1	D2	D3	D4	D5
Lean angle (degree)	Lower bound	-1	-1	-1	-1	-1
	Upper bound	1	1	1	1	1
Sweep angle (degree)	Lower bound	-1	-1	-1	-1	-1
	Upper bound	1	1	1	1	1
Chord scale factor	Lower bound	0.95	0.95	0.95	0.95	0.95
	Upper bound	1.05	1.05	1.05	1.05	1.05

Objective functions

The optimization this study presents had three objective functions, including the pressure ratio, isentropic efficiency and compressor mass flow rate. The formula of the compressor isentropic efficiency and pressure ratio are respectively presented in the following. Y stands for specific heat ratio, P_0 for the total pressure and T_0 for stagnation temperature.

$$\eta = \frac{(P_{0 \text{ out}}/P_{0 \text{ in}})^{(\gamma-1)/\gamma} - 1}{T_{0 \text{ out}}/T_{0 \text{ in}} - 1}$$

$$PR = \frac{P_{0 \text{ out}}}{P_{0 \text{ in}}}$$

Design of experiment

Design of experiment is a scientific approach to perform a sensitivity analysis by making objective modifications in the influential factors in a process or product.

After World War II, the Allies found Japan's telephone system of low quality for long-term communication purposes. Headquarters of Allies recommended that Japan should establish research facilities similar to Bell Labs. Japan then established Electrical Communications Laboratories (ECL) and Dr. Taguchi joined ECL to improve the productivity of the research and enhance the quality of the outcome. Taguchi noticed that industrial experiments had been enormously time-consuming and costly. So, focusing on minimizing the consumption of resources in experiments, he started developing new methods to optimize engineering experiments. His developments led to the establishment of some techniques known today as "Taguchi methods." Taguchi made a very influential contribution in the quality philosophy rather than the mathematical formulation of design of experiments. His quality philosophy created a unique and influential discipline for quality improvement that significantly varies from the older methods.¹⁷

In the Taguchi method, factor means a controllable variable that causes variability in response and is either qualitative or quantitative. In the operational phase, factors fall into three categories: signal factors, noise factors, and control factors. User or consumer sets signal factors in order to achieve the desired response. Noise factors are costly and difficult to control. The designer sets control factors, and this is also the designer who determines their appropriate values.

Taguchi believes that the key to achieving quality improvement is reducing variability. Thus, he recommends minimizing the amount of variability and producing not according to fixed tolerance.

The Taguchi method employs orthogonal arrays (L_n ; L stands for the orthogonal array itself and n stands for the number of studies or experiments) for the design of experiment. The appropriate array is chosen based on the number of variables. The process of design of experiment includes choosing the suitable orthogonal arrays, assigning factors to their suitable columns and determining the assumptions of the experiments. In orthogonal arrays, the columns present the parameters that should be optimized and the rows are the performed experiments. Outputs of the Taguchi experiments

are analyzed in multiple standard phases. The effects of factors are quantitatively assessed. The optimization and the optimized performance are determined based on the impact of factors.

In every L_n orthogonal array, each column has one degree of freedom. Thus, the number of columns of an array is determined by the number of freedom degrees of leading factors in an occasion. In an orthogonal array, no factor weighs more than other factors, and all levels of optimization variables are weighted equally across a column. Concerning that there were 15 design variables in this Taguchi-based study, the $L_{16}(2^{15})$ orthogonal array was employed, i.e., 16 two-level experiments on 15 design variables, and a sensitivity analysis was run on the objective functions by L_{32} orthogonal array (17). Based on the factorial method, there should be 215 experiments done to investigate the effect of 15 variables in two levels that high computational expenses make the process impossible. However, the Taguchi method provides with an accurate sensitivity analysis that only runs 16 experiments. In this study, every column of an array was assigned to one optimization variable; so, every array has 15 columns. Variables 1 to 5 are of the lean angle of 20, 40, 60, 80, and 100-percent spans. Variables 6 to 10 are related to the sweep angle of the aforementioned spans, and variables 11 to 15 relate to scale factor of the exact same spans. Every row of an array was assigned to an experiment. Values of design variables were determined to modify the geometry. Concerning that the orthogonal array is two-level in its every row, values of variables vary from 1 to 2. 1 represents the minimum value of the set, i.e., the lower bound, and 2 represents the maximum value of the set, i.e., the upper bound. The arrays mentioned above are shown in Figure 15. The Minitab app extracted the orthogonal array used in this study, and in doing so, the database was generated. Figure 16 is an example of one of the geometries created based on the array L_{16} by modifying distribution of the lean and sweep angle and chord of the base geometry.

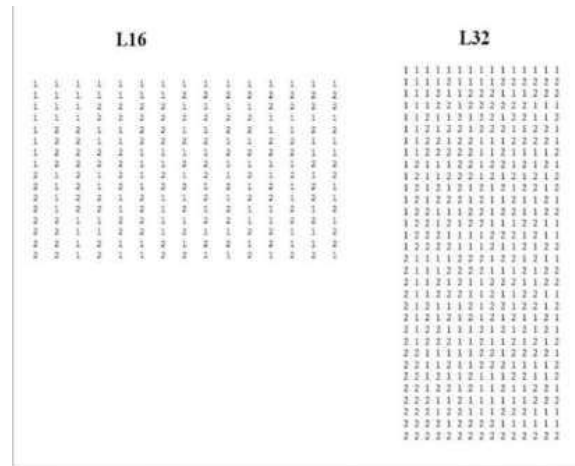


Figure 15 – Taguchi's L_{16} and L_{32} orthogonal arrays

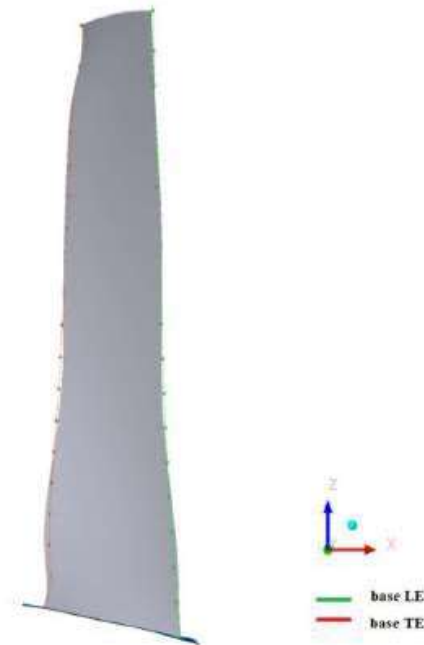


Figure 16 – The 15th geometry, L₁₆ array from the meridional surface view

In every experiment, values of optimization variables were determined based on values in the columns of the arrays. Then, a new geometry was created by varying the model geometry. The new geometry is then meshed by Turbogrid. A 3D CFD analysis is performed on the new geometry after setting the boundary conditions and specifications of the analysis in CFX. Values of objective functions including mass flow rate, pressure ratio and isentropic efficiency of fan are calculated and saved in the database. CFX, TurboGrid and Matlab programs are coupled during this coding process.

The 15 design variables are named by alphabets A to O, and the 32 values of experiments were named by y_1 to y_{32} which the subscript number represents the number of the experiments. The mean of variables of performance optimization is calculated through the following formula.

$$\bar{A}_1 = \frac{\sum y_i}{n} \quad \bar{A}_2 = \frac{\sum y_i}{n}$$

A_1 is the mean of objective functions of experiments in which A, i.e. the variable, has the minimum value, and A_2 is the mean of objective functions of experiments in which A has the maximum value. n represents the number of experiments.

In the following formula, T represents the sum of objective function in experiments and n_{tot} the total number of experiments.

$$T = \sum_{i=1}^{n_{tot}} y_i$$

CF represents the correction factor in the following formula.

$$CF = \frac{T^2}{n_{tot}}$$

S represents sum of the squares of each parameter's factors; for example, S_A shows the sum of squares of the variable A.

$$S_A = \frac{A_1^2}{n_{A1}} + \frac{A_2^2}{n_{A2}} - CF$$

In the following formula, P represents the participation percentage of each parameter.

$$P_A = \frac{S_A}{\sum S} \times 100$$

Results

After values of objective functions were determined in every experiment, the database was completed. Forty-eight experiments were performed to run the sensitivity analysis. The participation percentages of optimization variables were calculated for every objective function. Figures 17 to 19 present the effects of design variables on the three objective functions.

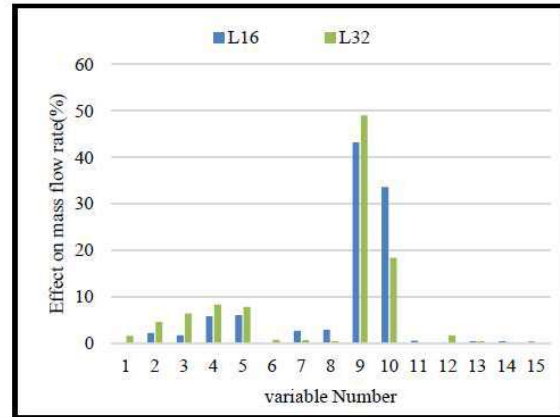


Figure 17 – Sensitivity of fan mass flow rate to design variables

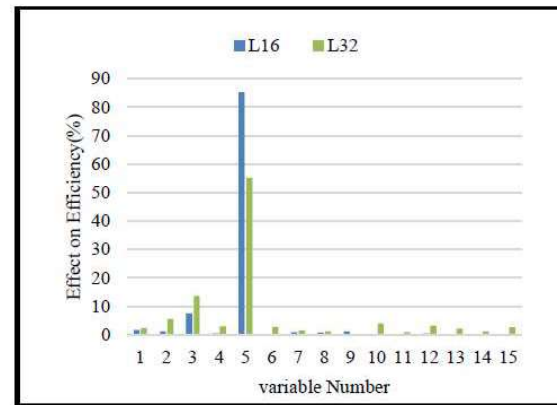


Figure 18 – Sensitivity of fan isentropic efficiency to design variables

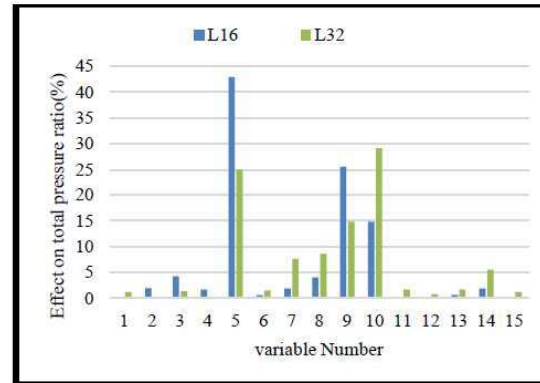


Figure 19 – Sensitivity of fan total pressure ratio to design variables

Figures 17 to 19 show that the most influential variables in objective functions are the same in arrays L16 and L32. This proves the reliability of the results because, according to the Taguchi theory, an increase of the number of experiments and levels

can change the participation percentage of variables, but the participation percentage of the variables with the most variance should not change.¹⁷ For example, in the sensitivity analysis of mass flow rate, variables 9 and 10 are the key variables in both arrays, although their participation percentage in array L_{16} equals 43 and 33 and 49 and 18 percent in array L_{32} , respectively. However, in the sensitivity analysis of pressure ratio, variable 5 was the most influential variable in array L_{16} , and variable 10 had the highest participation percentage in array L_{32} . Variables 5, 9, and 10 were the most significant variables of the fan pressure ratio

Conclusion

This paper concludes that the lean variable has the most effect on the isentropic efficiency (an 85 percent effect of the lean angle in span 100) and the sweep variable on the fan mass flow rate (a 43 and a 33 percent effect of sweep angle in span 80 and 100 respectively). The pressure ratio showed sensitivity to both variables (a 42 percent effect for blade lean in span 100 and a 25 percent effect for blade sweep in span 80). Assuming a fixed number of blades, degree of incidence, and camber angle, chord length distribution does not significantly affect objective functions compared to lean and sweep of the blade.

Research implications

The number of blades can be defined as a design variable and stall margin defined as objective functions, thereby investigating the effects of design variables on objective functions. Since variables 5, 9 and 10 had the highest participation percentage regarding the examined objective functions of this study, it is appropriate that the upper and lower bound of these variables would be increased during Optimization process, thereby eliminating or limiting the range of insignificantly influential variables.

References

[1] Wilson, Alec, et al. "Multidisciplinary Optimization of a Transonic Fan for Low Tone Noise." 17th AIAA/CEAS Aeroacoustics Conference (32nd AIAA Aeroacoustics Conference). 2011.

- [2] J. Denton , L. Xu ", THE EFFECTS OF LEAN AND SWEEP ON TRANSONIC FAN PERFORMANCE," ASME TURBO EXPO,2002.
- [3] E. Benini ", Three-Dimensional Multi-Objective Design Optimization of a Transonic Compressor Rotor," JOURNAL OF PROPULSION AND POWER,2004.
- [4] A. Oyama , M.-S. Liou ", Transonic Axial-Flow Blade Optimization: Evolutionary Algorithms/Three-Dimensional Navier–Stokes Solver," JOURNAL OF PROPULSION AND POWER, 2004.
- [5] C.-M. JANG, P. LI , K.-Y. KIM ", Optimization of Blade Sweep in a Transonic Axial Compressor Rotor," JSME International Journal,2005.
- [6] A. Samad , K.-Y. Kim ", Multi-objective optimization of an axial compressor blade," Journal of Mechanical Science and Technology 22, 2008.
- [7] S. R. Razavi , M. Boroomand ", Numerical and Performance Analysis of one row Transonic Rotor with Sweep and Lean angle," Journal of Thermal Science, 2014.
- [8] Siller, U. and Aulich, M., 2010, October. Multidisciplinary 3d-optimization of a fan stage performance map with consideration of the static and dynamic rotor mechanics. In Turbo Expo: Power for Land, Sea, and Air (Vol. 44021, pp. 317-328).
- [9] Siller, U., Voß, C. and Nicke, E., 2009, January. Automated multidisciplinary optimization of a transonic axial compressor. In 47th AIAA Aerospace Sciences Meeting Including The New Horizons Forum and Aerospace Exposition (p. 863).
- [10] M. Neshat, M. Akhlaghi, A. Fathi , H. Khaledi, "Investigation the effect of the blade sweep and lean in one stage of an industrial gas turbine's transonic compressor," Propulsion and Power Research, 2015.
- [11] Deng, X., Guo, F., Liu, Y. and Han, P., 2013. Aeromechanical optimization design of a transonic fan blade. In ASME Turbo Expo 2013: Turbine Technical Conference and Exposition. American Society of Mechanical Engineers Digital Collection.
- [12] Chahine, C., 2018. Multidisciplinary design optimization of aero-engine fan blades (Doctoral dissertation, University of Oxford).
- [13] Gaffin, W.O., 1980. Engine component improvement: Performance improvement, JT9D-7 3.8 AR fan.
- [14] ANSYS ",ANSYS TurboSystem User's Guide",2013.
- [15] ANSYS Inc ",ANSYS CFX-Solver Theory Guide",2009.
- [16] Strazisar, Anthony J., et al. Laser anemometer measurements in a transonic axial-flow fan rotor. Lewis Research Center, 1989.
- [17] Roy, Ranjit K. A primer on the Taguchi method. Society of Manufacturing Engineers, 2010.